Acta Pharmacologica Sinica (2018) 39: 243–250
 1671-4083/18
www.nature.com/aps

Article

SOMCL-085, a novel multi-targeted FGFR inhibitor, displays potent anticancer activity in FGFR-addicted human cancer models

Xi-fei JIANG[1, #], Yang DAI[2, #], Xia PENG[2], Yan-yan SHEN[2], Yi SU[2], Man-man WEI[3], Wei-ren LIU[1], Zhen-bin DING[1], Ao ZHANG[2], Ying-hong SHI[1, *], Jing AI[2, *]

[1]Department of Liver Surgery, Liver Cancer Institute, Zhongshan Hospital, Fudan University, Key Laboratory of Carcinogenesis and Cancer Invasion of Ministry of Education, Shanghai 200032, China; [2]Division of Anti-Tumor Pharmacology, State Key Laboratory of Drug Research, Shanghai Institute of Materia Medica, Chinese Academy of Sciences, Shanghai 201203, China; [3]CAS Key Laboratory of Receptor Research, and Synthetic Organic & Medicinal Chemistry Laboratory (SOMCL), Shanghai Institute of Materia Medica, Chinese Academy of Sciences, Shanghai 201203, China

Abstract

Aberrant fibroblast growth factor receptor (FGFR) activation is found across a diverse spectrum of malignancies, especially those lacking effective treatments. SOMCL-085 is a novel FGFR-dominant multi-target kinase inhibitor. Here, we explored the FGFR-targeting anticancer activity of SOMCL-085 both *in vitro* and *in vivo*. Among a panel of 20 tyrosine kinases screened, SOMCL-085 potently inhibited FGFR1, FGFR2 and FGFR3 kinase activity, with IC_{50} values of 1.8, 1.9 and 6.9 nmol/L, respectively. This compound simultaneously inhibited the angiogenesis kinases VEGFR and PDGFR, but without obvious inhibitory effect on other 12 tyrosine kinases. In 3 representative human cancer cell lines with different mechanisms of FGFR activation tested, SOMCL-085 (20–500 nmol/L) dose-dependently inhibited FGFR1-3 phosphorylation and the phosphorylation of their key downstream effectors PLCγ and Erk. In 7 FGFR aberrant human cancer cell lines, regardless of the mechanistic complexity of FGFR over-activation, SOMCL-085 potently inhibited FGFR-driven cell proliferation by arresting cells at the G_1/S phase. In the FGFR1-amplified lung cancer cell line H1581 xenograft mice and FGFR2-amplified gastric cancer cell line SNU16 xenograft mice, oral administration of SOMCL-085 (25, 50 $mg \cdot kg^{-1} \cdot d^{-1}$) for 21 days substantially suppressed tumor growth without affecting their body-weight. These results suggest that SOMCL-085 is a potent multi-target FGFR inhibitor that inhibits the FGFR-dependent neoplastic phenotypes of human cancer cells *in vitro* and *in vivo*.

Keywords: human cancer; anticancer drug; SOMCL-085; receptor tyrosine kinase; FGFR; xenograft nude mouse model

Acta Pharmacologica Sinica (2018) 39: 243–250; doi: 10.1038/aps.2017.96; published online 14 Sep 2017

Introduction

The fibroblast growth factor receptor (FGFR) family of receptor tyrosine kinases (RTKs) comprises four members (FGFR1, FGFR2, FGFR3, and FGFR4) that share significant sequence homology. Receptor activation by FGFs initiates a cascade of intracellular events that activate major survival and proliferative signaling pathways mediating crucial physiological mechanisms, such as tissue and metabolic homeostasis, endocrine functions and wound repair[1-4].

Aside from their normal physiological roles described above, FGFs and FGFRs are emerging as oncogenes that drive proliferation in a significant proportion of human tumors and can also mediate resistance to both cytotoxic and targeted agents[1, 4]. Deregulation of FGFR signaling has been documented in a broad spectrum of tumor types, in the form of FGFR gene amplifications, somatic mutations, or translocations, especially in tumors lacking effective treatment[1-4]. For example, amplification of FGFR1 (8q12locus) is found in approximately 17% of squamous non-small cell lung carcinoma (NSCLC) cases[5, 6]. Amplification of FGFR2 has been described in 5%–10% of gastric cancer cases, particularly of the aggressive diffuse subtype[7], and in 4% of triple-negative breast cancer cases[8]. Mutations in FGFR3 are frequent in non-muscle invasive urothelial cell carcinomas and

# These authors contributed equally to this work.
*To whom correspondence should be addressed.
E-mail jai@simm.ac.cn (Jing AI);
shi.yinghong@zs-hospital.sh.cn (Ying-hong SHI)
Received 2017-05-24 Accepted 2017-06-20

are also found in approximately 15% of high-grade invasive urothelial cancers[9, 10]. Thus, FGFR has been validated as an attractive target for cancer treatment.

Several FGFR inhibitors are undergoing clinical studies, but none of them have yet been approved for clinical use[4]. Many of the published FGFR inhibitors approved for VEGFR2-based antiangiogenic therapies retain significant activity against VEGFR but have less potency against FGFRs[4, 11-15]. Their activity against VEGFR is the likely source of grade 3/4 hypertension induction and the dose-limiting toxicity of these inhibitors[16-19]. Most importantly, the angiogenesis-regulating kinase VEGFR, PDGFR, and FGFR pathways are able to compensate for each other when single pathways are inhibited[20-23]. Accordingly, more recent treatments have focused on inhibiting multiple signaling pathways simultaneously.

Given the facts mentioned above, we sought to develop an orally bioavailable, FGFR-dominant kinase inhibitor that simultaneously inhibits VEGFR and PDGFR. To this end, we developed a novel triple kinase inhibitor of FGFR, VEGFR, and PDGFR, SOMCL-085. In the present study, we evaluated the FGFR-targeting antitumor activity of SOMCL-085 both *in vitro* and *in vivo*. The compound potently inhibited FGFR kinase activity and FGFR signal transduction, thereby suppressing the FGFR-dependent neoplastic phenotype of tumor cells. In xenografts of human lung and gastric tumor cell lines with FGFR-driven gene alterations, SOMCL-085 administration led to significant antitumor activity at well-tolerated doses. Our results suggest that SOMCL-085 has promising therapeutic potential for the treatment of FGFR-driven cancer in patients who acquire resistance to anti-VEGF/VEGFR2-based therapies.

Materials and methods

Compound

SOMCL-085 [6-((2-(4-(4-(2-hydroxyethyl)piperazin-1-yl)benzamido)pyridin-4-yl)oxy)-*N*-methyl-1-naphthamide hydrochloride] (Figure 1) was synthesized in Prof Ao ZHANG's Laboratory at the Shanghai Institute of Materia Medica. SOMCL-085 was dissolved in dimethyl sulfoxide at 10 mmol/L and subsequently serially diluted to specific concentrations.

ELISA kinase assay

The effects of SOMCL-085 on the activities of various tyrosine kinases were determined using enzyme-linked immunosorbent assays (ELISAs) with purified recombinant proteins. Briefly, 20 μg/mL poly (Glu, Tyr) $_{4:1}$ (Sigma, St Louis, MO, USA) was pre-coated in 96-well plates as a substrate. A 50 μL aliquot of 10 μmol/L ATP solution diluted in kinase reaction buffer [50 mmol/L HEPES (pH 7.4), 50 mmol/L $MgCl_2$, 0.5 mmol/L $MnCl_2$, 0.2 mmol/L Na_3VO_4, and 1 mmol/L DTT] was added to each well; 1 μL of the indicated compound diluted in 1% DMSO (*v*/*v*) (Sigma, St Louis, MO, USA) was then added to each reaction well. DMSO (1%, *v*/*v*) was used as the negative control. The kinase reaction was initiated by the addition of purified tyrosine kinase proteins diluted in 49 μL of kinase reaction buffer. After incubation for 60 min at 37 °C, the plate was washed three times with phosphate-buffered saline (PBS) containing 0.1% Tween 20 (T-PBS). Anti-phosphotyrosine (PY99) antibody (100 μL; 1:500, diluted in 5 mg/mL BSA T-PBS) was then added. After a 30-min incubation at 37 °C, the plate was washed three times, and 100 μL of horseradish peroxidase-conjugated goat anti-mouse IgG (1:1000, diluted in 5 mg/mL BSA T-PBS) was added. The plate was then incubated at 37°C for 30 min and washed three times. A 100-μL aliquot of a solution containing 0.03% H_2O_2 and 2 mg/mL *o*-phenylenediamine in 0.1 mol/L citrate buffer (pH 5.5) was added. The reaction was terminated by the addition of 50 μL of 2 mol/L H_2SO_4 as the color changed, and the plate was analyzed using a multi-well spectrophotometer (SpectraMAX190, from Molecular Devices, Palo Alto, CA, USA) at 490 nm. The inhibition rate (%) was calculated using the following equation: $[1-(A_{490}/A_{490\ control})] \times 100\%$. The IC_{50} values were calculated from the inhibition curves in two separate experiments.

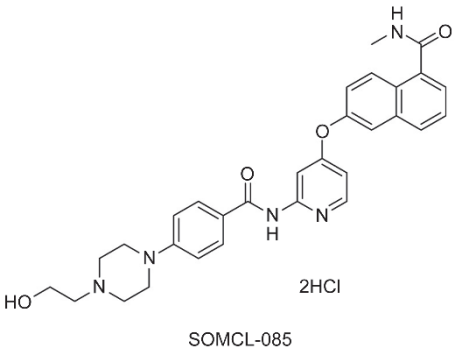

SOMCL-085

Figure 1. The chemical structure of SOMCL-085.

Cell culture

Human lung cancer cell line NCI-H1581, human acute myelogenous leukemia cell line KG1, human gastric cancer cell lines SNU16 and KATOIII, and human bladder cancer cell line NCI-H716 were purchased from the American Type Culture Collection (ATCC, Manassas, VA, USA). Human bladder cancer cell line RT112 was purchased from the DSMZ-German collection of microorganisms and cell cultures. Human bladder cancer cell line UMUC14 was purchased from the European Collection of Cell Cultures (ECACC). All the cell lines were routinely maintained in media according to the suppliers' recommendations and authenticated via short tandem repeats analysis by Genesky Biopharma Technology (last tested in 2016).

Western blot analysis

KG1, SNU16 and UMUC14 cells were treated with the indicated dose of SOMCL-085 for 2 h at 37 °C and then lysed in 1×SDS sample buffer. The cell lysates were subsequently resolved by 10% SDS-PAGE and transferred to nitrocellulose membranes. The membranes were probed with the appropriate primary antibodies [phospho-FGFR, FGFR1, FGFR2,

FGFR3, phospho-ERK, ERK, PLCγ, phospho–PLCγ, tubulin (all from Cell Signaling Technology, Beverly, MA, USA)], and then with horseradish peroxidase-conjugated anti-rabbit or anti-mouse IgG. The immune reactive proteins were detected using an enhanced chemiluminescence detection reagent (Thermo Fisher Scientific, Rockford, IL, USA).

Cell proliferation assays

Cells were seeded in 96-well plates at a low density in growth media. The next day, appropriate controls or designated concentrations of compounds were added to each well, and the cells were incubated for 72 h. Finally, cell proliferation was determined using a sulforhodamine B (SRB) assay or a cell counting kit (CCK-8) assay. IC_{50} values were calculated by concentration-response curve fitting using a SoftMax pro-based four-parameter method.

Cell cycle analysis

The effects of compounds on cell cycle progression and population distribution were determined by flow cytometry. Cells were seeded at 2×10^5 cells in 6-well plates and treated with compounds at the indicated concentration or with vehicle as a control. After 24 h, the cells were collected, fixed and stained with propidium iodide (10 μg/mL) for 30 min and then analyzed using a flow cytometer (FACSCalibur instrument; Becton, Dickinson & Co, USA). Data were plotted using CellQuest software (Becton, Dickinson & Co, USA).

In vivo antitumor activity assay

Female nude mice (4–6-weeks old) were housed and maintained under specific pathogen-free conditions. Animal procedures were performed according to the institutional ethical guidelines for animal care. Tumor cells at a density of 5×10^6 in 200 μL were injected subcutaneously (sc) into the right flank of nude mice and then allowed to grow to 700–800 mm^3, which was defined as a well-developed tumor. Subsequently, the well-developed tumors were cut into 1-mm^3 fragments and transplanted sc into the right flank of nude mice using a trocar. When the tumor volume reached 100–150 mm^3, the mice were randomly assigned into either a vehicle control group (n=12) or a treatment group (n=6 per group). The control group was given only vehicle (water for injection), while the treatment groups received SOMCL-085 at the indicated doses via oral injection once daily for 2–3 weeks. The sizes of the tumors were measured twice per week using a microcaliper. Tumor volume (TV)=(length×width^2)/2, and the individual relative tumor volume (RTV) was calculated as follows: RTV = V_t/V_0, where V_t was the volume on a particular day and V_0 was the volume at the beginning of the treatment. The RTV was shown on indicated days as the median RTV±SE indicated for groups of mice. Percent (%) inhibition (TGI) values were measured on the final day of study for the drug-treated mice compared with vehicle-treated mice and were calculated as $100 \times \{1-[(V_{\text{Treated Final day}}-V_{\text{Treated Day 0}})/(V_{\text{Control Final day}}-V_{\text{Control Day 0}})]$. Significant differences between the treated and control groups ($P\leq0.05$) were determined using the Student's t test.

Results

SOMCL-085 is a potent FGFR-dominant kinase inhibitor that simultaneously inhibits VEGFR and PDGFR

SOMCL-085 (Figure 1) was selected for further characterization based on screens designed to identify a triple inhibitor of FGFR, VEGFR, and PDGFR. SOMCL-085 potently inhibited FGFR1–3 kinase activity, with IC_{50} values of 1.8, 1.9 and 6.9 nmol/L, respectively (Figure 2, Table 1), and displayed weaker activity against FGFR4 (IC_{50}=319.9 nmol/L) (Figure 2, Table 1). Simultaneously, SOMCL-085 significantly inhibited VEGFR1, VEGFR2, PDGFR-α, and PDGFR-β kinase activity, with potency that was equal or lower than that observed against FGFR1–3. By contrast, no obvious inhibitory effect was observed against the other 12 tyrosine kinases tested from different families (Table 1). These data indicated that SOMCL-085 is a potent FGFR-dominant kinase inhibitor that simultaneously inhibits VEGFR and PDGFR. Here, we explored the *in vitro* and *in vivo* anti-FGFR activity of SOMCL-085. The pharmacologic properties of SOMCL-085 in models associated with PDGFR and KDR will be described elsewhere.

SOMCL-085 blocks FGFR activation and downstream signaling in cancer cells

To further evaluate the cellular activity of SOMCL-085 targeting FGFR kinase, we analyzed its effects on the phosphorylation of FGFR and its major downstream signaling molecules, PLCγ and ERK[1]. Three representative human cancer cell lines with different mechanisms of FGFR activation were used, including FGFR1-translocated myeloid leukemia cancer cell line KG-1, FGFR2-amplified gastric cancer cell

Table 1. The kinase panel screening data of SOMCL-085.

Kinase	IC_{50} (nmol/L)[a]
FGFR1	1.8±0.2
FGFR2	1.9±0.4
FGFR3	6.9±1.2
FGFR4	319.9±24.9
VEGFR-1	5.6±0.5
VEGFR-2	1.2±0.2
PDGFR-α	22.6±10.5
PDGFR-β	7.8±1.8
EGFR	>1000
ErbB2	>1000
ErbB4	>1000
ABL	>1000
c-Src	>1000
EPH-A2	>1000
IGF1R	>1000
ALK	>1000
LTK	>1000
ROS1	>1000
c-Met	>1000
AXL	>1000

[a]Values are the mean±SD of two independent assays.

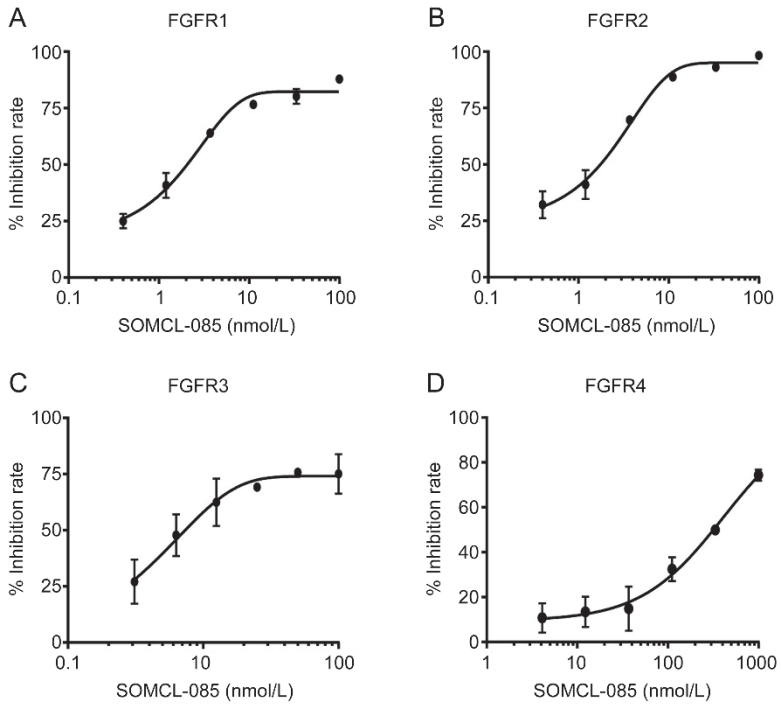

Figure 2. SOMCL-085 potently inhibited FGFR1, FGFR2, and FGFR3 kinase activity. The inhibition curve of SOMCL-085 against FGFR1 (A), FGFR2 (B), FGFR3 (C), and FGFR4 (D) kinase activity using ELISA assay.

line SNU16, and FGFR3-mutated bladder cancer cell line UMUC14. SOMCL-085 showed significant inhibition of FGFR1–3 phosphorylation in a dose-dependent manner in the individual cancer cell lines. The phosphorylation of ERK and PLCγ was also clearly inhibited (Figure 3A–C). Thus, SOMCL-085 potently inhibits FGFR signaling, regardless of the mechanistic complexity of FGFR activation.

SOMCL-085 elicits significant effects against FGFR1–3-driven cancer cell proliferation via G_1/S cell cycle arrest

To elucidate the impact of SOMCL-085 on FGFR-mediated cancer cell proliferation, seven cancer cell lines harboring the frequently occurring oncogenic forms of different FGFR members were chosen: FGFR1-translocated KG1 cells, FGFR1-amplified NCI-H1581 cells, FGFR2-amplified SNU16 cells, KATOIII cells, NCI-H716 cells, FGFR3-amplified RT112 cells, and FGFR3-mutated UMUC14 cells. The ability of SOMCL-085 to inhibit cell proliferation in these cells over a 3-day period was assessed using standard SRB and CCK8 proliferation assays. As shown in Figure 4A–G and Table S1, SOMCL-085 strongly inhibited FGFR1-, FGFR2-, and FGFR3-driven cancer cell proliferation in a dose-dependent manner. The concentrations of SOMCL-085 required to inhibit cellular FGFR phosphorylation were in good agreement with the *in vitro* proliferation IC_{50} values (Table S1, Figure 3, Figure 4A–G), indicating that SOMCL-085 inhibited the tested cancer cell proliferation via targeted FGFR signaling.

FGFR inhibition is known to exert anti-proliferative effects

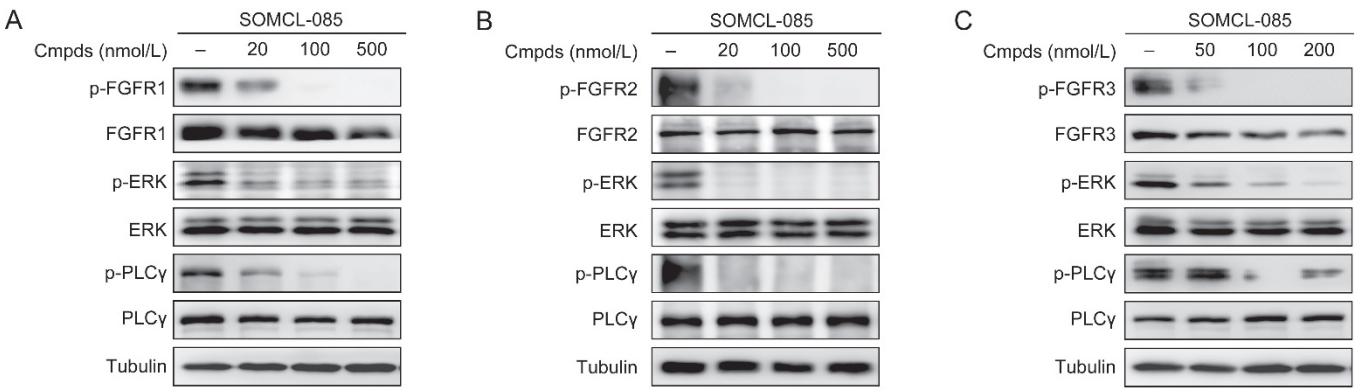

Figure 3. SOMCL-085 effectively inhibits the phosphorylation of FGFR and the downstream effectors Erk and PLCγ in KG-1, SNU16, and UMUC14 cells. KG1 (A), SNU16 (B) or UMUC14 (C) cells treated with SOMCL-085 for 2 h at the indicated concentrations were lysed, and subjected to Western blot analysis.

by arresting cells in the G_1/S phase[24]. To further confirm cellular FGFR targeting activity, we used a FGFR3-mutant UMUC14 cancer cell line as the representative FGFR-addicted context to measure cell-cycle distribution upon SOMCL-085 treatment. As expected, UMUC14 cells showed dramatic increases in the G_1 phase population upon treatment with SOMCL-085 (Figure 4H), with no increases in the sub-G_1 population (data not shown), further confirming that the potent anti-proliferative activity of the compound in the FGFR-addicted context was the result of targeted FGFR signaling.

SOMCL-085 significantly inhibits FGFR-mediated tumor growth *in vivo* at well-tolerated doses

To assess the *in vivo* antitumor efficacy of SOMCL-085, the FGFR1-amplified lung cancer cell line NCI-H1581 and the FGFR2-amplified gastric cancer cell line SNU16 xenograft mouse models were used. In the SNU16 model, SOMCL-085 was orally administered once daily at doses of 25 or 50 mg/kg for 21 consecutive days. The results showed that SOMCL-085 could suppress tumor growth in a dose-dependent manner, with tumor growth inhibition rates of 62.9% and 81.3% at doses of 25 mg/kg and 50 mg/kg, respectively (Figure 5A–C). Additionally, SOMCL-085 was well tolerated, with no significant body-weight loss in any of the treatment groups (Figure 5D). Similar results were observed in the NCI-H1581 model treated with SOMCL-085 (Figure 5E–H). These results indicated that SOMCL-085 elicited robust antitumor efficacy in FGFR-dependent tumor models at well-tolerated doses. Therefore, SOMCL-085 is a potential multi-target FGFR inhibitor for further drug development.

Discussion

Recent clinical success in molecular-targeted therapies for cancer based on the identification of oncogenic gene alterations

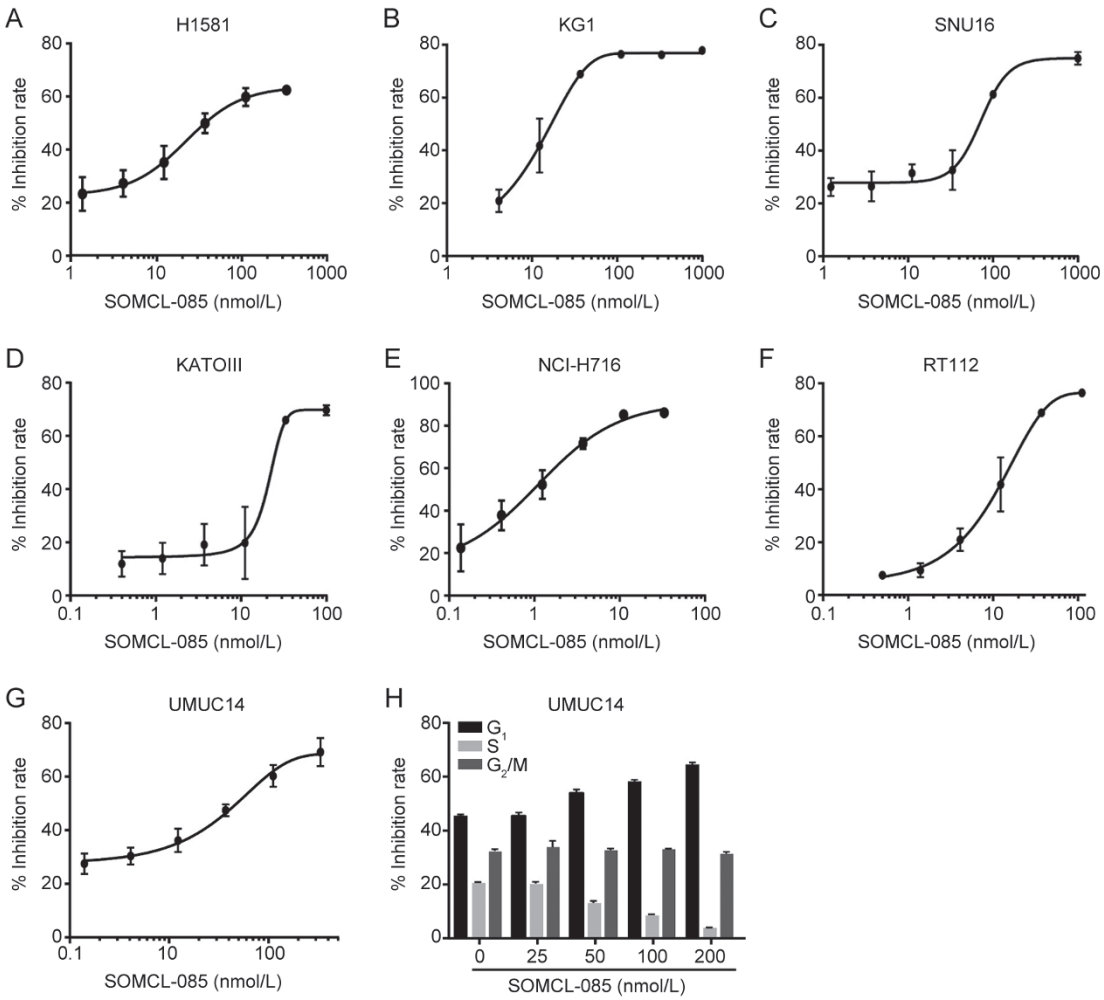

Figure 4. SOMCL-085 elicits significant effects against FGFR1–3–driven cancer cell proliferation via G_1/S cell cycle arrest. (A–G) The anti-proliferative activity of SOMCL-085 against a panel of tumor cell lines, including NCI-H1581 (A), KG1 (B), SNU16 (C), KATOIII (D), NCI-H716 (E), RT112 (F), UMUC14 (G), was determined by a sulforhodamine B (SRB) assay or a CCK-8 assay. The inhibit rates were plotted as the mean±SD from two independent experiments. (H) SOMCL-085 induced G_1/S phase cell cycle arrest in FGFR–addicted UMUC14 cancer cells. UMUC14 cells were treated with the indicated concentrations of SOMCL-085 for 24 h. The percentages of cells in different cell cycle phases determined by FACS and analyzed with Modifit LT were plotted. The data shown are the mean±SD from three independent experiments.

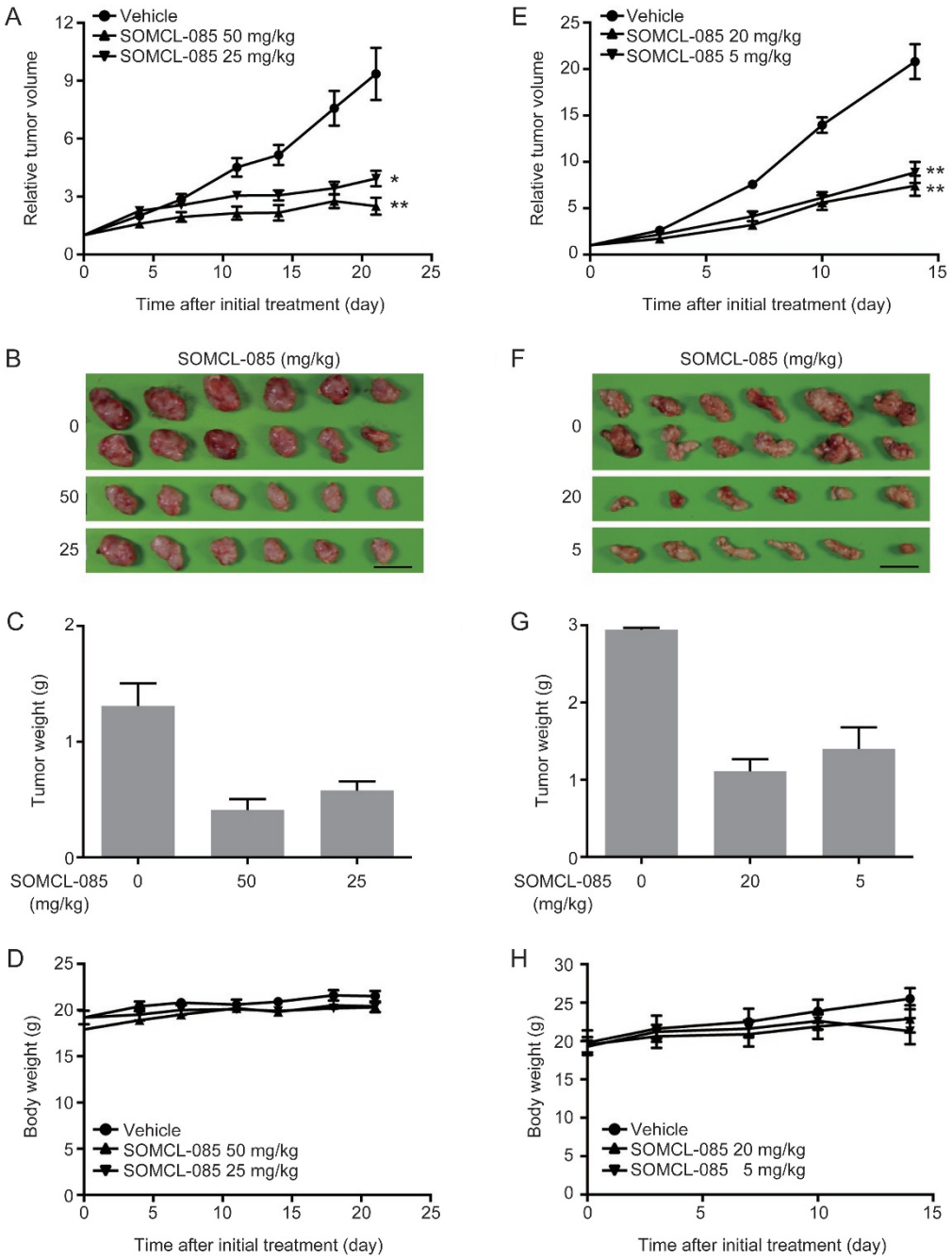

Figure 5. SOMCL-085 significantly inhibits FGFR-mediated tumor growth *in vivo* at well-tolerant doses. (A–D) Antitumor efficacy of SOMCL-085 in SNU16 xenograft model. (A) Tumor growth inhibition upon SOMCL-085 treatment in SNU16 xenografts was shown. The RTVs are expressed as the mean± SEM. Significant difference from the vehicle group was determined using a *t*-test, $^{*}P<0.05$, $^{**}P<0.01$. Representative image of tumors (scale bar = 20 mm) (B) and tumor weights (C) were shown on day 21 after mice injected with SOMCL-085. (D) Body weight measurements during the treatment. (E–H) Antitumor efficacy of SOMCL-085 in NCI-H1581 xenograft model. (E) Tumor growth inhibition upon SOMCL-085 treatment in NCI-H1581 xenografts was shown. The RTVs are expressed as the mean±SEM. Significant difference from the vehicle group was determined using a *t*-test, $^{**}P<0.01$. Representative image of tumors (scale bar=20 mm) (F) and tumor weights (G) were shown on day 14 after mice injected with SOMCL-085. (H) Body weight measurements during the treatment.

and their specific inhibitors has been associated with dramatic antitumor effects, reduced side effects, and improved patient survival. Mutant FGFR, a clinically relevant molecular oncogenic driver, is found across a diverse spectrum of malignancies, especially those lacking effective treatment[1, 2, 4]. Aberrant FGFR activation is closely associated with tumor formation and metastasis, as well as resistance to approved therapies[4, 25-30]. Therefore, inhibiting FGFR signaling could have significant potential for the treatment of human cancers driven by FGFR over-activation.

Here, we report the activity of the multi-targeted kinase inhibitor, SOMCL-085, against the FGFR family of kinases. Using FGFR-dependent cancer cells with different mechanisms of activation, we showed that SOMCL-085 potently inhibits the activation of FGFR1–3 signaling in cells and significantly inhibits cancer cell proliferation. Consistent with anti-proliferative effects mediated by inhibition of individual FGFRs, phosphorylation of the receptor was inhibited in all three cell lines with similar potency. In addition, using FGFR1-amplified H1581 and FGFR2-amplified SNU16 mouse xenograft models, we showed that daily oral administration of SOMCL-085 led to substantial inhibition of tumor growth at well-tolerated doses. Our study supports SOMCL-085 as a potent FGFR inhibitor that inhibits the activity of FGFRs regardless of their mechanism of activation.

It cannot be ignored that, as a FGFR-targeted inhibitor, SOMCL-085 simultaneously inhibits the angiogenesis kinases VEGFR and PDGFR. Although antiangiogenic therapies have proven to be effective in clinical settings, they also have well-characterized serious side effects that limit their clinical application. Most importantly, angiogenic kinase pathways including VEGFR, PDGFR, and FGFR can easily compensate for each other during blockade of a single pathway[20-23, 30]. All of these findings suggest that a multi-targeting strategy towards both FGFR and VEGFR with PDGFR would provide a better treatment opportunity for patients who have disease progression following anti-VEGF/VEGFR2-based therapies. SOMCL-085 is an FGFR-dominant inhibitor with simultaneous inhibitory effects on VEGFR and PDGFR that may have promising treatment potential for patients who acquire resistance to anti-VEGF/VEGFR2-based therapies.

In summary, SOMCL-085 is a multi-targeted kinase inhibitor that displays potent pan-FGFR activity and inhibits the growth of cancer cells containing FGFR activated by multiple mechanisms. Several cancer indications contain genomic aberrations in FGFRs, and patients with these diseases tend to lack effective targeted therapies. These data strongly support the investigation of SOMCL-085 as a therapy for patients with FGFR-driven cancers

Acknowledgements
This work was supported by funds from the National Natural Science Foundation of China (No 81473243), grants from the Science and Technology Commission of Shanghai Municipality (No 17431902900) and grants from the "Personalized Medicines–Molecular Signature-based Drug Discovery and Development", Strategic Priority Research Program of the Chinese Academy of Sciences (No XDA12020000).

Author contribution
Jing AI and Ying-hong SHI designed the study; Xi-fei JIANG, Yang DAI, Yan-yan SHEN, Yi SU, Xia PENG, Wei-ren LIU, and Zhen-bin DING performed the research; Man-man WEI and Ao ZHANG contributed new reagents or analytic tools; Xi-fei JIANG, Xia PENG, and Jing AI analyzed the data; Xi-fei JIANG, Xia PENG, and Jing AI wrote the paper.

Supplementary information
Supplementary information is available at the website of Acta Pharmacologica Sinica.

References
1 Turner N, Grose R. Fibroblast growth factor signalling: from development to cancer. Nat Rev Cancer 2010; 10: 116–29.
2 Dieci MV, Arnedos M, Andre F, Soria JC. Fibroblast growth factor receptor inhibitors as a cancer treatment: from a biologic rationale to medical perspectives. Cancer Discov 2013; 3: 264–79.
3 Touat M, Ileana E, Postel-Vinay S, Andre F, Soria JC. Targeting FGFR Signaling in Cancer. Clin Cancer Res 2015; 21: 2684–94.
4 Babina IS, Turner NC. Advances and challenges in targeting FGFR signalling in cancer. Nat Rev Cancer 2017; 17: 318–32.
5 Yang W, Yao YW, Zeng JL, Liang WJ, Wang L, Bai CQ, *et al.* Prognostic value of FGFR1 gene copy number in patients with non-small cell lung cancer: a meta-analysis. J Thoracic Dis 2014; 6: 803–9.
6 Weiss J, Sos ML, Seidel D, Peifer M, Zander T, Heuckmann JM, *et al.* Frequent and focal FGFR1 amplification associates with therapeutically tractable FGFR1 dependency in squamous cell lung cancer. Sci Translation Med 2010; 2: 62ra93.
7 Matsumoto K, Arao T, Hamaguchi T, Shimada Y, Kato K, Oda I, *et al.* FGFR2 gene amplification and clinicopathological features in gastric cancer. Br J Cancer 2012; 106: 727–32.
8 Turner N, Lambros MB, Horlings HM, Pearson A, Sharpe R, Natrajan R, *et al.* Integrative molecular profiling of triple negative breast cancers identifies amplicon drivers and potential therapeutic targets. Oncogene 2010; 29: 2013–23.
9 Helsten T, Elkin S, Arthur E, Tomson BN, Carter J, Kurzrock R. The FGFR Landscape in cancer: analysis of 4,853 tumors by next-generation sequencing. Clin Cancer Res 2016; 22: 259–67.
10 Cappellen D, De Oliveira C, Ricol D, de Medina S, Bourdin J, Sastre-Garau X, *et al.* Frequent activating mutations of FGFR3 in human bladder and cervix carcinomas. Nat Genet 1999; 23: 18–20.
11 Roth GJ, Heckel A, Colbatzky F, Handschuh S, Kley J, Lehmann-Lintz T, *et al.* Design, synthesis, and evaluation of indolinones as triple angiokinase inhibitors and the discovery of a highly specific 6-methoxycarbonyl-substituted indolinone (BIBF 1120). J Med Chem 2009; 52: 4466–80.
12 Bhide RS, Cai ZW, Zhang YZ, Qian L, Wei D, Barbosa S, *et al.* Discovery and preclinical studies of (*R*)-1-(4-(4-fluoro-2-methyl-1*H*-indol-5-yloxy)-5- methylpyrrolo[2,1-f][1,2,4]triazin-6-yloxy)propan- 2-ol (BMS-540215), an *in vivo* active potent VEGFR-2 inhibitor. J Med Chem 2006; 49: 2143–6.
13 Wedge SR, Kendrew J, Hennequin LF, Valentine PJ, Barry ST, Brave SR, *et al.* AZD2171: a highly potent, orally bioavailable, vascular endothelial growth factor receptor-2 tyrosine kinase inhibitor for the treatment of cancer. Cancer Res 2005; 65: 4389–400.
14 Huynh H, Ngo VC, Fargnoli J, Ayers M, Soo KC, Koong HN, *et al.* Brivanib alaninate, a dual inhibitor of vascular endothelial growth factor receptor and fibroblast growth factor receptor tyrosine kinases, induces growth inhibition in mouse models of human hepatocellular carcinoma. Clin Cancer Res 2008; 14: 6146–53.
15 Sarker D, Molife R, Evans TR, Hardie M, Marriott C, Butzberger-Zimmerli P, *et al.* A phase I pharmacokinetic and pharmacodynamic study of TKI258, an oral, multitargeted receptor tyrosine kinase inhibitor in patients with advanced solid tumors. Clin Cancer Res 2008; 14: 2075–81.

16 Herbst RS. Toxicities of antiangiogenic therapy in non-small-cell lung cancer. Clin Lung Cancer 2006; 8 Suppl 1: S23–30.
17 Izzedine H, Ederhy S, Goldwasser F, Soria JC, Milano G, Cohen A, *et al.* Management of hypertension in angiogenesis inhibitor-treated patients. Ann Oncol 2009; 20: 807–15.
18 Ricciardi S, Tomao S, de Marinis F. Toxicity of targeted therapy in non-small-cell lung cancer management. Clin Lung Cancer 2009; 10: 28–35.
19 Shojaei F, Ferrara N. Role of the microenvironment in tumor growth and in refractoriness/resistance to anti-angiogenic therapies. Drug Resistance Updates 2008; 11: 219–30.
20 Zhao Y, Adjei AA. Targeting angiogenesis in cancer therapy: moving beyond vascular endothelial growth factor. Oncologist 2015; 20: 660–73.
21 Batchelor TT, Duda DG, di Tomaso E, Ancukiewicz M, Plotkin SR, Gerstner E, *et al.* Phase II study of cediranib, an oral pan-vascular endothelial growth factor receptor tyrosine kinase inhibitor, in patients with recurrent glioblastoma. J Clin Oncol 2010; 28: 2817–23.
22 Casanovas O, Hicklin DJ, Bergers G, Hanahan D. Drug resistance by evasion of antiangiogenic targeting of VEGF signaling in late-stage pancreatic islet tumors. Cancer Cell 2005; 8: 299–309.
23 Abdollahi A, Folkman J. Evading tumor evasion: current concepts and perspectives of anti-angiogenic cancer therapy. Drug Resistance Updates 2010; 13: 16–28.
24 Liu H, Ai J, Shen A, Chen Y, Wang X, Peng X, *et al.* c-Myc Alteration determines the therapeutic response to FGFR inhibitors. Clin Cancer Res 2017; 23: 974–84.
25 Fernanda Amary M, Ye H, Berisha F, Khatri B, Forbes G, Lehovsky K, *et al.* Fibroblastic growth factor receptor 1 amplification in osteosarcoma is associated with poor response to neo-adjuvant chemotherapy. Cancer Med 2014; 3: 980–7.
26 Ware KE, Marshall ME, Heasley LR, Marek L, Hinz TK, Hercule P, *et al.* Rapidly acquired resistance to EGFR tyrosine kinase inhibitors in NSCLC cell lines through de-repression of FGFR2 and FGFR3 expression. PLoS One 2010; 5: e14117.
27 Yadav V, Zhang X, Liu J, Estrem S, Li S, Gong XQ, *et al.* Reactivation of mitogen-activated protein kinase (MAPK) pathway by FGF receptor 3 (FGFR3)/Ras mediates resistance to vemurafenib in human B-RAF V600E mutant melanoma. J Biol Chem 2012; 287: 28087–98.
28 Manchado E, Weissmueller S, Morris JP, Chen CC, Wullenkord R, Lujambio A, *et al.* A combinatorial strategy for treating KRAS-mutant lung cancer. Nature 2016; 534: 647–51.
29 Kim B, Wang S, Lee JM, Jeong Y, Ahn T, Son DS, *et al.* Synthetic lethal screening reveals FGFR as one of the combinatorial targets to overcome resistance to Met-targeted therapy. Oncogene 2015; 34: 1083–93.
30 Terai H, Soejima K, Yasuda H, Nakayama S, Hamamoto J, Arai D, *et al.* Activation of the FGF2-FGFR1 autocrine pathway: a novel mechanism of acquired resistance to gefitinib in NSCLC. Mol Cancer Res 2013; 11: 759–67.